Available online at www.sciencedirect.com
ScienceDirect
Journal of Photochemistry and Photobiology A: Chemistry 182 (2006) 319–324
Journal of Photochemistry and Photobiology A:Chemistry
www.elsevier.com/locate/jphotochem

Rapid prototyping of silica glass microstructures by the LIBWE method: Fabrication of deep microtrenches

Yoshizo Kawaguchi *, Tadatake Sato, Aiko Narazaki, Ryozo Kurosaki, Hiroyuki Niino

Photonics Research Institute (PRI), National Institute of Advanced Industrial Science and Technology (AIST), Tsukuba Central 5, 1-1-1 Higashi, Tsukuba 305-8565, Japan

Abstract

We have constructed a system for surface-microstructuring transparent materials, such as silica glass, using laser-induced backside wet etching (LIBWE), which includes an excimer laser and a mask projection system. In this report, we describe the advantages of the LIBWE method and present various results showing deep microtrenches fabricated using this method. We examine the applicability of this method to rapid prototyping, and propose a mechanism for the formation of deep microtrenches.

Keywords: Silica glass; Surface-microstructuring; Nanosecond-pulsed UV laser; Microtrench; Rapid prototyping

1. Introduction

Silica glass has excellent properties: exceptional transparency in the deep ultraviolet (DUV)–visible (VIS)–near infrared (NIR) region, mechanical hardness, thermal stability, durability against chemicals, etc. Micro-/nano-fabrication of silica glass is a key technology for a number of applications: micro-optics, optoelectronics devices, photonics devices, microfluidic devices for high throughput chemical synthesis, chemical and biological analysis, etc. However, the above properties and the mechanical brittleness make micromachining of silica glass very difficult.

In industrial fabrication processes, a combination of photo- or electron-beam lithography and etching either in a plasma or a strong acid, typically HF, is utilized [1–3]. However, these methods require elaborate process sequences and utilities, including, for example, the coating and removal of resist layers and vacuum systems for plasma etching equipment. Typical etch rate in plasma etching or HF etching is around 0.5 $\mu m\,min^{-1}$ at maximum. Therefore, more effective, simpler and faster methods of fabricating devices on silica glass substrates have been pursued, and various researchers have studied the micro-/nano-fabrication of silica glass using lasers [4–38]. The following methods have been reported: use of a tightly focused conventional ultraviolet (UV) laser [4], vacuum ultraviolet (VUV) lasers [5–8], CO_2 lasers [9], laser plasma soft-X-rays [10], focused femtosecond (fs) lasers [11–14], and laser-induced plasma-assisted ablation (LIPAA) [15,16]. The method we have developed is laser-induced backside wet etching (LIBWE) [17–38].

A schematic diagram illustrating the LIBWE method, especially for deep microetching, is shown in Fig. 1. A nanosecond (ns)-pulsed UV laser beam passes through a photomask and a transparent plate to be absorbed by a dye solution located at the rear surface of the plate. Due to strong laser absorption by the solution, the laser energy is initially confined to a photo-activated micron scale thin layer at the interface between the transparent plate and the solution, where the dye molecules are excited collectively. The photo-activated layer interacts with the surface of the plate, resulting in microetching. Typical etch rate is around 10 $nm\,pulse^{-1}$, indicating that as large as about 1 $\mu m\,s^{-1}$ is possible with the repetition rate of around 100 Hz, about two order larger than ordinary plasma etching or HF etching.

The LIBWE method has several advantages, which are listed below:

(i) resist-free, single-step process in atmospheric conditions with a simple pre-/post-treatment [18,20,21];

* Corresponding author. Tel.: +81 29 861 4564; fax: +81 29 861 4560.
E-mail address: y-kawaguchi@aist.go.jp (Y. Kawaguchi).

1010-6030/$ – see front matter © 2006 Elsevier B.V. All rights reserved.
doi:10.1016/j.jphotochem.2006.05.033

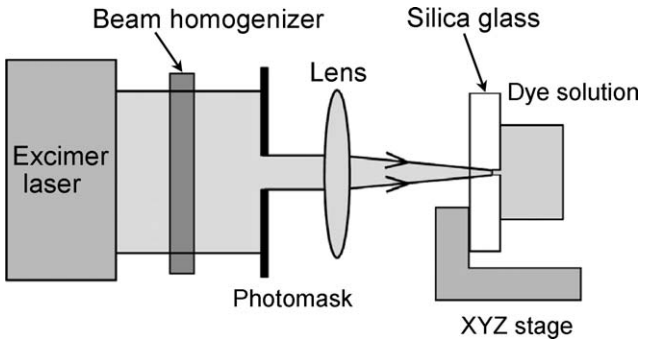

Fig. 1. Experimental setup for the fabrication of deep microtrenches on silica glass using the LIBWE method.

(ii) control of etch depth from the nanometer scale to several hundreds of micrometers by controlling the laser conditions such as fluence and number of laser pulses [18,20,21,23,24,28,34,37];
(iii) about two orders large etch rate at maximum compared to ordinary industrial methods, plasma etching or HF etching;
(iv) etching of various transparent materials including silica glass and sapphire [17–38];
(v) flexible surface structuring by use of a mask projection system [26].

Of these advantages, the ability to fabricate trenches with depths of several hundreds of micrometers is one of the most prominent characteristics of the LIBWE method. In this paper, we have revisited the LIBWE method for fabricating these deep microtrenches. We give detailed results for etching silica glass and discuss the mechanism by which successful deep etching is achieved. Using the LIBWE method, a 420 μm deep, 7 μm wide microtrench (aspect ratio = 60) was successfully fabricated with an irradiation time of about 5 min, indicating that this method can be very effective for rapid prototyping of transparent materials in practical use.

2. Experimental

A synthetic silica glass plate (Tosoh SGM, ES grade, thickness ≈2.0 mm) was used for etching. For the dye solution, a saturated pyrene/acetone solution was employed: the concentration was about 0.4 mol dm^{-3}. A KrF excimer laser (Lambda Physik, EMG-201MSC, λ = 248 nm, FWHM ≈ 30 ns) and a mask projection system (MicroLas, ValioLas) including a homogenizer were used in the LIBWE process (Fig. 1). The laser fluence was set to $F = 1.0\,J\,cm^{-2}$. The photomask was comprised of slits to enable fabrication of 1 mm long trenches with widths 7 or 9 μm.

A sample holder was placed on a XYZ stage (Sigmatech Co., FS-1050). The position of the sample was controlled with a resolution of ±0.2 μm. Because of the limited depth-of-focus (DOF) of the projection lens, in the case of deep microetching, the silica plate was moved away from the lens after irradiation of a certain number of laser pulses in order that the etch front, i.e., the interface between the silica surface and the solution, remained within the DOF of the projection lens (Fig. 1).

For a more precise study of the effect of an out of focus beam on the etch depth and quality, we fabricated trenches where the distance between the silica plate and the projection lens differed by 22.5 μm for each trench. This was done by oblique incidence of the laser beam on the substrate. The beam was applied at an angle of 13° with respect to the normal to the solid–liquid interface. A photomask designed to produce microtrenches 10 μm wide and 1 mm in length, and with an interval of 100 μm between them was used. The irradiation was done using a KrF excimer laser beam delivering 3000 pulses at $F = 1.5\,J\,cm^{-2}$ at a repetition rate of 20 Hz. A saturated pyrene/acetone solution was used as a laser-absorbing liquid, and the focal point was fixed while etching proceeded.

After deep etching, the samples were rinsed, cut perpendicular to the trench, and the cross-sectional structures were observed by scanning electron microscopy (SEM, Keyence VE-7800).

In addition, in order to examine the quality of the sidewalls, we fabricated a polymer replica by injection molding and made observations using an SEM. A microtrench array was fabricated on the silica glass with the following conditions: a photomask designed to produce an array of trenches of, width = 10 μm, length = 1 mm, and interval of 100 μm was used in the process; KrF excimer laser irradiation delivering 12,000 pulses at a fluence of $F = 0.7\,J\,cm^{-2}$ and repetition rate of 50 Hz was carried out; a saturated pyrene/acetone solution was used for the dye solution; the silica plate was moved further away from the projection lens five times in 8 μm steps for each 1000 pulses and seven times in 10 μm steps for each subsequent 1000 pulses. A replica of the deep microtrench array was prepared using a resin (Struers, Repliset F-5). The pre-polymer was mixed with a curing agent, placed immediately on the microtrench array, and set inside a vacuum chamber. The chamber was quickly pumped for less than 1 min and then returned to atmospheric pressure. The sample was kept for several tens of minutes at room temperature to cure the resin. The peeled off replica was observed using a SEM.

3. Results and discussion

3.1. Results of deep microtrenches on silica glass

Basically, a width of a trench is determined by a slit width, and an etch rate is affected by a fluence in the LIBWE method. Using a saturated pyrene/acetone solution for the laser-absorbing liquid, 80 μm deep and 10 μm wide trenches with a duty ratio of 10 were etched in silica glass using a KrF excimer laser delivering 12,000 pulses at a fluence of $0.7\,J\,cm^{-2}$ and repetition rate of 50 Hz. The etched trenches are shown in Fig. 2(a). A cross-sectional SEM image of the structure shows good quality microtrenches with straight and parallel sidewalls, and the image of the polymer replica (Fig. 2(b)) shows the quality of the sidewalls to be reasonable.

The results of microtrench fabrication on silica glass using the LIBWE method were strongly (Fig. 3) dependent on the laser irradiation conditions. Fig. 3(a) shows the etch depth versus the number of laser pulses for microtrenches of 9 μm × 1 mm fabricated under different stage control conditions: condition (1),

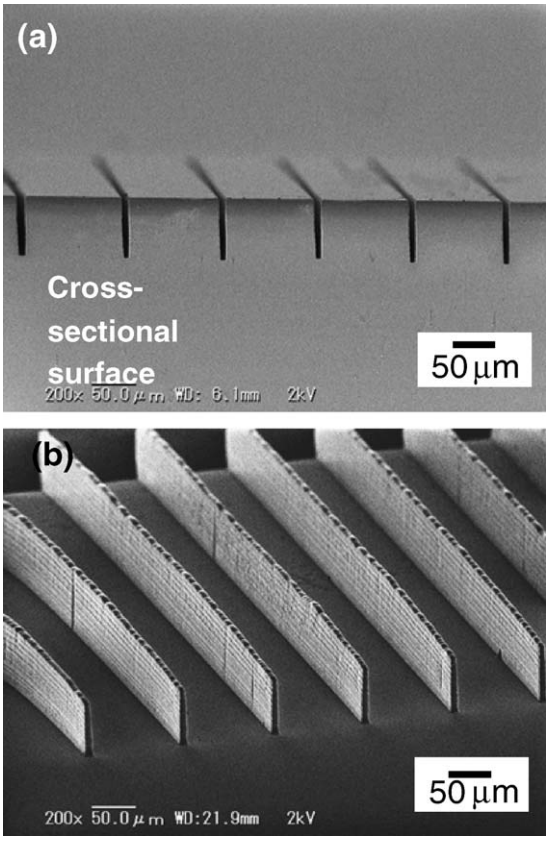

Fig. 2. (a) Cross-sectional SEM image of an array of deep trenches on a silica surface. The widths are 10 μm, depths 80 μm, and the duty ratio is 10. The trench array was fabricated using 12,000 pulses of KrF excimer laser irradiation at a fluence $F = 0.7\,\mathrm{J\,cm^{-2}}$ and repetition rate of 50 Hz. The absorbing medium was a saturated pyrene/acetone solution, and the silica plate was moved away from the lens five times by 8 μm for each 1000 pulses followed by seven times by 10 μm for each of the next 1000 pulses, (b) SEM image of a replica of the deep trench array on a polymer surface.

stage moved 10 μm for every 1000 pulses; condition (2), stage moved 10 μm for every 2000 pulses. Under condition (1), the etch depth increased with increasing pulse number even beyond 20,000 pulses, while for condition (2), the etch depth almost saturated at around 10,000 pulses. The movement of the stage in case (2) corresponds to $5\,\mathrm{nm\,pulse^{-1}}$. With this slow rate of movement, the etch front progressively became further out of focus. On the other hand, in case (1), the etch depth increased at a progressively faster rate than the movement of the stage: for example, 48 μm for a stage movement of 40 μm and irradiation of 4000 pulses, 133 μm for a stage movement of 100 μm and irradiation of 10,000 pulses, and as much as 300 μm for a stage movement of only 200 μm and irradiation of 20,000 pulses. The initial etch rate was estimated to be $12\,\mathrm{nm\,pulse^{-1}}$ by the data points obtained under irradiation of up to 8000 pulses, while the etch rate observed between 16,000 and 20,000 pulses was $16\,\mathrm{nm\,pulse^{-1}}$. It shows that the etch rate increases with pulse number, maybe due to a confinement effect by the deep sidewalls, and that the margin for the out of focus condition is very large in deep microetching. Fig. 3(b) is a cross-sectional SEM image of a microtrench fabricated under condition (1) and irradiated with 20,000 pulses, and Fig. 3(c) shows one fabricated under condition (2) and irradiated with 10,000 pulses. Although the sidewalls of the trench in Fig. 3(c) was less straight than that in Fig. 3(b), the deep trenches were, nevertheless, acceptable for ones fabricated in such an out of focus process.

To observe the effect of an out of focus laser beam on microetching using the LIBWE method, the silica plate was irradiated with the laser beam at an oblique angle of incidence such that the distance between the projection lens and each adjacent trench on the plate differed by 22.5 μm. The trenches were fabricated simultaneously using a photomask designed to produce 10 μm wide trenches at intervals of 100 μm. The plate was irradiated with a KrF excimer laser beam delivering 3000 pulses at $F = 1.5\,\mathrm{J\,cm^{-2}}$ and a repetition rate of 20 Hz at an angle of 13° with respect to the normal to the solid–liquid interface. A saturated pyrene/acetone solution was used as the laser-absorbing liquid, and the focal point was fixed while etching proceeded. In this condition, the distance between the projection lens and each adjacent trench on the silica plate differed by 22.5 μm (100 μm × sin 13° = 22.5 μm.). Fig. 4(a and b) show cross-sectional SEM images of the trenches at different magnifications. As can clearly be seen in Fig. 4(a), there were nine etched trenches. The difference in distance from the lens to the trenches at each end was 180 μm (= 22.5 μm × 8 intervals), although the etch depth was at its maximum for the central trench and decreased for trenches moving progressively away from the center in both directions. This means that the LIBWE method works even when the position of the sample is about 40–50 μm away from the focal point of the present projection lens, enabling successful deep microetching. A magnified view of the deepest microtrench is shown in Fig. 4(c). The microtrench was fabricated satisfactorily with a depth of about 70 μm after irradiation of 3000 pulses, in spite of the oblique angle of incidence.

Following the above results, a good quality 7 μm wide and 420 μm deep trench was successfully fabricated. This is shown in Fig. 5 and plotted by a solid circle in Fig. 3(a): the sample was moved 15 μm for every 1000 pulses of irradiation, corresponding to a rate of $15\,\mathrm{nm\,pulse^{-1}}$ and 25,000 pulses were delivered at 80 Hz. To our knowledge, such deep microtrenches cannot be fabricated using other methods, because other etching methods are based on the difference in etch rates between the resist and the substrate; at present there are no resists that can withstand the etch times required for such deep etching. The etch depth, 420 μm, was again much greater than the distance the silica plate was moved during irradiation of 25,000 pulses, which was 375 μm. A large DOF of about ±50 μm widens the process margin and favors fabrication of deep microtrenches of several hundreds of micrometers in depth in the LIBWE method, though accurate tracking of the center of the imaging area is difficult and the process parameters should be carefully checked beforehand in order to etch deep microtrenches to accurate depths.

3.2. Mechanism of deep microetching on silica glass by the LIBWE method

Based on the molar absorption coefficient of a dilute pyrene solution, the optical penetration depth is estimated

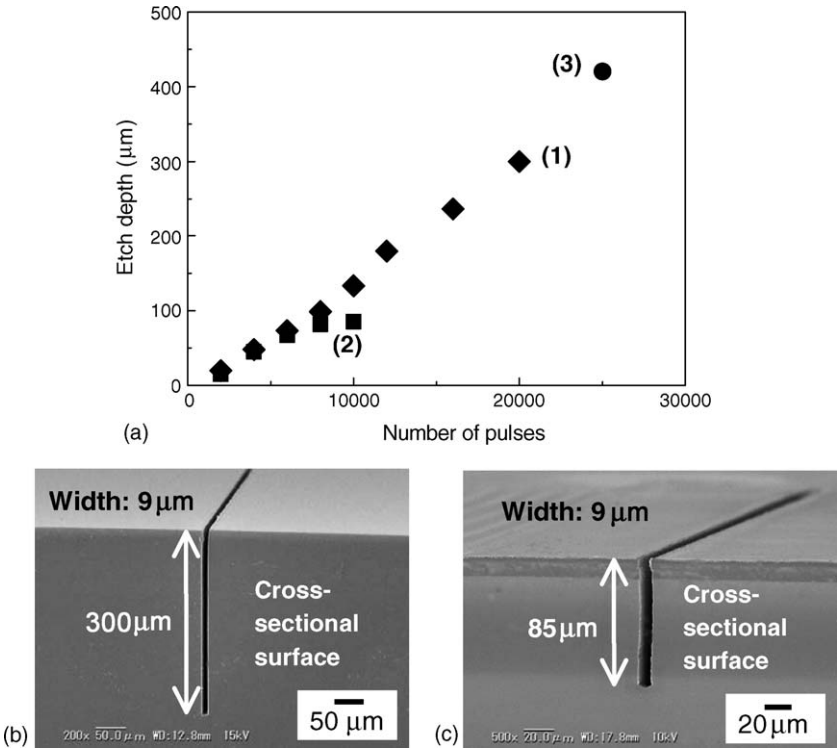

Fig. 3. (a) Dependence of the etch depth on the pulse number for silica glass microtrenches under KrF excimer laser irradiation at a fluence $F = 1.0\,\mathrm{J\,cm^{-2}}$ using a saturated pyrene/acetone solution with three different conditions: (1) slit width ≈9 μm on the sample, repetition rate = 10 Hz, and the silica plate was moved away from the lens by 10 μm for every 1000 pulses; (2) slit width ≈9 μm on the sample, repetition rate = 10 Hz, and the silica plate was moved away from the lens by 10 μm for every 2000 pulses; (3) slit width ≈7 μm on the sample, repetition rate = 80 Hz, and the silica plate was moved away from the lens by 15 μm for every 1000 pulses, corresponding to the trench shown in Fig. 5. (b) Cross-sectional SEM image of a deep trench fabricated by irradiation of 20,000 pulses under condition (1) in 'a'. (c) Cross-sectional SEM image of a deep trench fabricated by irradiation of 10,000 pulses under condition (2) in 'a'.

to be $D = 0.7$ μm for acetone solution containing pyrene at $0.4\,\mathrm{mol\,dm^{-3}}$. This means that most of the laser energy is deposited in the solution less than 1 μm away from the surface of the silica. The thinness of the laser-induced photo-activated region of the organic solution contributes to the fabrication of the deep microtrenches by preventing damage to the already etched sidewalls. In addition, as the laser beam is incident from the back surface through the transparent glass substrate, the photo-activated process occurs effectively at the etch front of the trench. On the other hand, a laser incident from the front surface of the

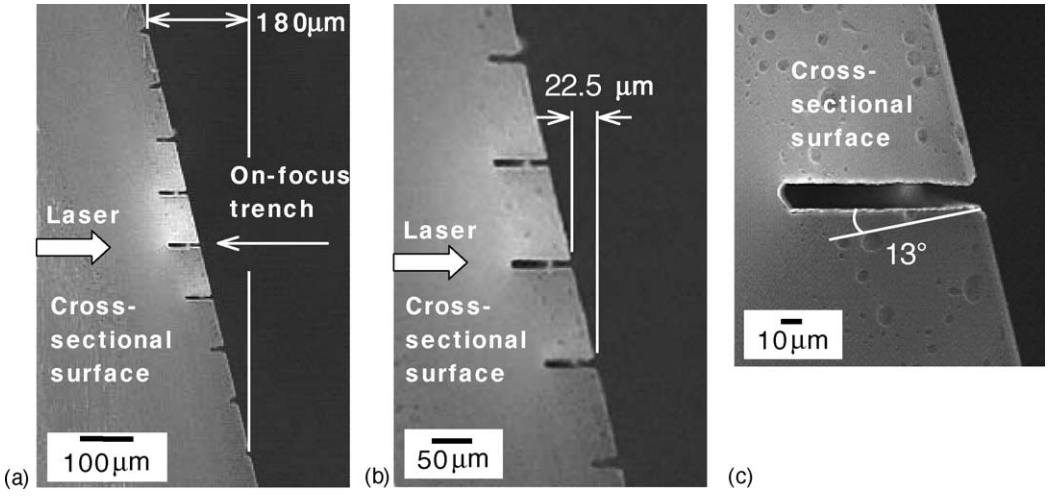

Fig. 4. (a) Cross-sectional SEM images of trenches on silica glass fabricated by the LIBWE method where the distance between each adjacent trench on the plate and the projection lens differed by 22.5 μm due to the oblique incidence of the laser beam. The photomask used during etching was designed to produce trenches with widths of 10 μm, lengths of 1 mm, and intervals of 100 μm between them. A KrF excimer laser beam delivering 3000 pulses at $F = 1.5\,\mathrm{J\,cm^{-2}}$ and repetition rate of 20 Hz was used at an angle of 13° with respect to the normal of the solid–liquid interface. A saturated pyrene/acetone solution was used as a laser-absorbing liquid. The focal point was fixed while etching proceeded. (b) Magnified view of 'a'. (c) Magnified view of the deepest oblique trench in 'a', about 70 μm in depth.

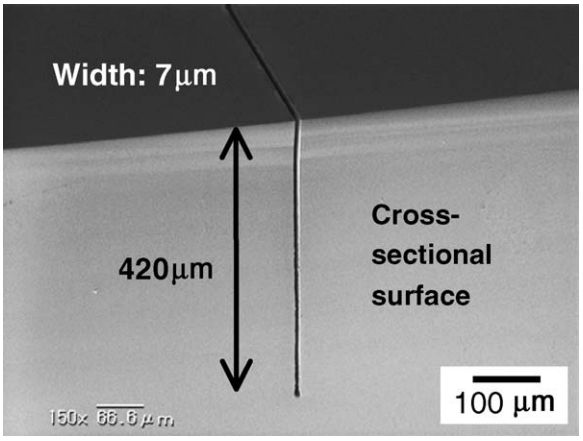

Fig. 5. Cross-sectional SEM image of a deep trench, 420 μm in depth and 7 μm in width, fabricated using 25,000 pulses of KrF excimer laser irradiation at a fluence $F = 1.0\,J\,cm^{-2}$ and repetition rate of 80 Hz, with saturated pyrene/acetone solution as the laser-absorbing medium. The silica plate was moved away from the lens by 15 μm for every 1000 pulses, condition (3) in Fig. 3 (a).

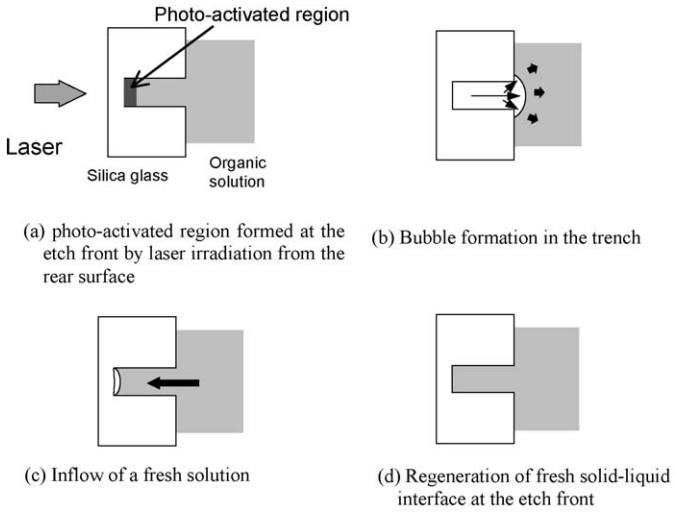

Scheme 1. (a–d) Proposed possible mechanism for fabrication of deep microtrenches by the LIBWE method.

material can easily result in the formation of tapered trenches [39], reflecting the track of the focused laser beam.

Furthermore, Ishii and co-workers reported time-resolved shadowgraph images of a pyrene/acetone ($0.4\,mol\,dm^{-3}$) solution under KrF excimer laser irradiation with 300 μm in beam diameter and $F = 0.5\,J\,cm^{-2}$ [40,41]. According to their report, the bubble expanded hemispherically with a maximum radius of about 700 μm (the maximum volume $V_{max} \approx 7.2 \times 10^8\,\mu m^3$ with 300 μm in beam diameter) at a delay time of 70 μs. We assume that the maximum volume of the bubble is proportional to the deposited laser energy, i.e., irradiated area times laser fluence. Then, the corresponding volume of vapor bubble is estimated to be $1.4 \times 10^8\,\mu m^3$ at $F = 1.0\,J\,cm^{-2}$ on the etching area of 7 μm × 1 mm. This corresponding volume of vapor bubble is more than one order larger than the volume of the deepest trench in the silica glass ($V = 7$ μm width × 1 mm length × 420 μm depth $= 2.9 \times 10^6\,\mu m^3$). This means that the maximum size of the vapor bubble would be expanded above the trench volume.

From above discussions, the following model is proposed for explaining the successful fabrication of deep microetching by the LIBWE method, as depicted in Scheme 1.

(i) Laser irradiation from the back surface, and very thin laser-induced photo-activated region of the organic solution.
(ii) Bubble formation in the trench by laser-induced vaporization of the solution.
(iii) Inflow of a fresh solution into the trench.
(iv) Regeneration of fresh solid–liquid interface at the etch front.

That is, the irradiated laser-energy is confined to a very thin photo-activated region at the etch front for every pulse of the laser beam, causing etching of typically around $10\,nm\,pulse^{-1}$. The local etching will prevent damage to the already etched sidewalls (Scheme 1(a)).

Photo-absorption of the organic solution follows vaporization and formation of a bubble for every irradiation of the laser pulse. The bubble expands large enough to expel etched fragments and photo-activated solutions outside the etched trench (Scheme 1(b)). This also works effectively to prevent deposition of the fragments onto the sidewalls.

After expansion, the bubble collapses by cooling within a several tens of μs. Inflow of a fresh solution into the trench takes place (Scheme 1(c)). Regeneration of the fresh solid–liquid interface is performed by a recoil pressure [42] at the etch front at the bottom of the trench (Scheme 1(c)). The fresh solution at the etch front is excited by the next pulse of laser irradiation (Scheme 1(d)). Thus, deep trench structures are fabricated in silica glass by multiple irradiation of the laser beam.

4. Conclusion

We have described surface-microstructuring of silica glass by the LIBWE method with short irradiation times, which opens up the possibility of the rapid prototyping of microstructures on silica glass. Especially, the peculiar characteristics of the LIBWE method enable fabrication of very deep microtrenches on silica glass, more than 100 μm deep, which with other methods are too difficult to fabricate. With the combination of high horizontal resolution, the LIBWE method can be applied to the fabrication of three-dimensional microstructured devices made of silica glass. The microtrench structures fabricated using the LIBWE method can also be very effectively used for the formation of replicas in polymers, making this a useful tool in the fabrication of polymer microdevices.

Acknowledgements

This study was partly supported by the Center of Excellence (COE) Development Program on Photoreaction Control and Photofunctional Materials from Ministry of Education, Culture, Sports, Science and Technology of Japan and by Industrial Tech-

nology Research Grant in 2006 from New Energy and Industrial Technology Development Organization (NEDO) of Japan.

References

[1] A. Somashekhar, S. O'Brien, J. Electrochem. Soc. 143 (1996) 2885.
[2] T. Furusawa, Y. Horiike, Jpn. J. Appl. Phys. 42 (2003) 4009.
[3] I. Steingoetter, A. Grosse, H. Fouckhardt, SPIE Proc. 4984 (2003) 234.
[4] J. Ihlemann, Appl. Surf. Sci. 54 (1992) 193.
[5] R. Herman, R.S. Marjoribanks, A. Oettl, K. Chen, Appl. Surf. Sci. 154–155 (2000) 577.
[6] J. Ihlemann, S. Müller, S. Puschmann, D. Schäfer, M. Wei, J. Li, P.R. Herman, Appl. Phys. A 76 (2003) 751.
[7] K. Sugioka, S. Wada, H. Tashiro, K. Toyoda, A. Nakamura, Appl. Phys. Lett. 65 (1994) 1510.
[8] J. Zhang, K. Sugioka, T. Takahashi, K. Toyoda, K. Midorikawa, Appl. Phys. A 71 (2000) 23.
[9] N. Kitamura, K. Fukumi, J. Nishii, T. Kinoshita, N. Ohno, Jpn. J. Appl. Phys. 42 (2003) L712.
[10] T. Makimura, Y. Kenmotsu, H. Miyamoto, H. Niino, K. Murakami, Surf. Sci. 593 (2005) 248.
[11] H. Varel, D. Ashkenasi, A. Rosenfeld, M. Wahmer, E.E.B. Campbell, Appl. Phys. A 65 (1997) 367.
[12] K. Miura, J.R. Qiu, H. Inouye, T. Mitsuyu, K. Hirao, Appl. Phys. Lett. 71 (1997) 3329.
[13] A. Marcinkevicius, S. Juodkazis, M. Watanabe, M. Miwa, S. Matsuo, H. Misawa, J. Nishii, Opt. Lett. 26 (2001) 277.
[14] Y. Nakata, T. Okada, M. Maeda, Appl. Phys. A 77 (2003) 399.
[15] J. Zhang, K. Sugioka, K. Midorikawa, Opt. Lett. 23 (1998) 1486.
[16] J. Zhang, K. Sugioka, K. Midorikawa, Appl. Phys. A 69 (1999) S879.
[17] J. Wang, H. Niino, A. Yabe, Jpn. J. Appl. Phys. 38 (1999) L761.
[18] J. Wang, H. Niino, A. Yabe, Appl. Phys. A 68 (1999) 111.
[19] J. Wang, H. Niino, A. Yabe, Appl. Phys. A 69 (1999) S271.
[20] J. Wang, H. Niino, A. Yabe, Appl. Surf. Sci. 154–155 (2000) 571.
[21] J. Wang, H. Niino, A. Yabe, SPIE Proc. 3933 (2000) 347.
[22] Y. Yasui, H. Niino, Y. Kawaguchi, A. Yabe, Appl. Surf. Sci. 186 (2002) 552.
[23] X. Ding, Y. Yasui, Y. Kawaguchi, H. Niino, A. Yabe, Appl. Phys. A 75 (2002) 437.
[24] X. Ding, Y. Kawaguchi, H. Niino, A. Yabe, Appl. Phys. A 75 (2002) 641.
[25] H. Niino, Y. Yasui, X. Ding, A. Narazaki, T. Sato, Y. Kawaguchi, A. Yabe, J. Photochem. Photobiol. A: Chem. 158 (2003) 179.
[26] X. Ding, T. Sato, Y. Kawaguchi, H. Niino, Jpn. J. Appl. Phys. 42 (2003) L176.
[27] X. Ding, Y. Kawaguchi, T. Sato, A. Narazaki, H. Niino, Chem. Commun. (2003) 2168.
[28] Y. Kawaguchi, H. Niino, A. Yabe, in: A. Peled (Ed.), Photo-Excited Processes, Diagnostics and Applications—Fundamentals and Advanced Topics, Kluwer Academic Publisher, Boston, 2003, pp. 339–357.
[29] Y. Kawaguchi, X. Ding, A. Narazaki, T. Sato, H. Niino, Appl. Phys. A 79 (2004) 883.
[30] H. Niino, X. Ding, R. Kurosaki, A. Narazaki, T. Sato, Y. Kawaguchi, Appl. Phys. A 79 (2004) 827.
[31] X. Ding, Y. Kawaguchi, T. Sato, A. Narazaki, R. Kurosaki, H. Niino, J. Photochem. Photobiol. A: Chem. 166 (2004) 129.
[32] X. Ding, Y. Kawaguchi, T. Sato, A. Narazaki, R. Kurosaki, Langmuir 20 (2004) 9769.
[33] Y. Kawaguchi, X. Ding, A. Narazaki, T. Sato, H. Niino, Appl. Phys. A 80 (2005) 275.
[34] Y. Kawaguchi, T. Sato, A. Narazaki, R. Kurosaki, H. Niino, Jpn. J. Appl. Phys. 44 (2005) L176.
[35] T. Gumpenberger, T. Sato, R. Kurosaki, A. Narazaki, Y. Kawaguchi, H. Niino, Chem. Lett. (2006) 218.
[36] H. Niino, Y. Kawaguchi, T. Sato, A. Narazaki, T. Gumpenberger, R. Kurosaki, Appl. Surf. Sci. 252 (2006) 4387.
[37] Y. Kawaguchi, H. Niino, T. Sato, A. Narazaki, R. Kurosaki, J. Phys. Conf. Ser., submitted for publication.
[38] H. Niino, Y. Kawaguchi. T. Sato, A. Narazaki, T. Gumpenberger, R. Kurosaki, J. Phys. Conf. Ser., submitted for publication.
[39] A.A. Tseng, Y.-T. Chen, K.-J. Ma, Opt. Lasers Eng. 41 (2004) 827.
[40] D. Kumaki, K. Tsunoda, H. Yajima, T. Ishii, Proceedings of the Annual Meeting of the Japanese Photochemistry Association (Kanazawa City), September 2001 (in Japanese).
[41] $F = 0.5\,\mathrm{J\,cm^{-2}}$ is half fluence of what we used for microtrench etching using the LIBWE method.
[42] A. Vogel, W. Lauterborn, R. Timm, J. Fluid Mech. 206 (1989) 299.